# Numerical analysis of the dynamic frequency responses of damaged micro-lattice core sandwich plates

Matías Braun[1,2] , Inés Ivañez[3] and Josué Aranda-Ruiz[3]

## Abstract

In this work, a numerical analysis of the dynamic frequency responses of sandwich plates with micro-lattice core is presented. The finite element analysis is implemented in the commercial software Abaqus/Standard, calculating the natural frequencies and eigenmodes of sandwich plates containing defects on the micro-lattice structure. In order to include the presence of defects, an aleatory algorithm is developed in MATLAB. The effect of the damage percentage, cell type, cell size and material on the frequency and modal responses of the sandwich plates is highlighted. Results show that the dynamic frequency response may be useful for analysing practical issues related to non-destructive damage identification of imperfections in the micro-lattice core of sandwich structures.

## Introduction

In the last decades, the use of composite sandwich structures extended to different engineering fields, such as aerospace, automotive, maritime and military.[1–4] This type of structures can be used in a variety of engineering problems, where the strength-to-weight ratio represents an important factor in the design process.[5] The sandwich structures with aluminium honeycomb core have been widely used in aerospace applications, as a result of their superior mechanical properties, such as specific stiffness and specific strength.

Nevertheless, the principal limitations of this kind of closed cells are associated with the gas and moisture retentions.[6–8] In order to solve these disadvantages, many works have focused to optimise the design of open cells, such as the metallic lattice structures.[9] This work is centred on the study of open-cell cores, in particular on a new micro-lattice (ML) core material manufactured using selective laser melting.[10,11]

Many studies based on open-cell geometries have greatly focused on predicting theoretically, numerically and experimentally the macroscopic stiffness and strength.[12–16] The scanning electron microscope images of the ML structures, presented in Gümrük et al.,[12] showed that the structures are very complex and include imperfections which are semi-melted powders

over the surface of micro-struts and variable diameters. Note that these defects affect the mechanical responses of the ML structure.[17]

The presence of imperfections or damages in the structure produces changes in the stiffness that modify the vibration responses of the structure. Damage detection methods based on vibration can be performed as a real-time damage detection method to overcome the drawbacks of the common non-destructive testing (NDT) techniques. In the last three decades, a lot of researchers have focused on the study of damage detection based on vibration methods.[18–23]

In this study, to detect the presence of ML core defects, a non-destructive damage detection method[24,25] based on vibration responses is analysed. The main

[1]Departamento de Construcciones, Facultad de Ingeniería, Universidad Nacional de La Plata, Buenos Aires, República Argentina
[2]Consejo Nacional de Investigación Científicas y Técnicas (CONICET) CCT La Plata, Buenos Aires, República Argentina
[3]Department of Continuum Mechanics and Structural Analysis, University Carlos III of Madrid, Leganés, Spain

**Corresponding author:**
Matías Braun, Departamento de Construcciones, Facultad de Ingeniería, Universidad Nacional de La Plata, Calle 48 y 115 s/n, (B1900TAG) La Plata, Buenos Aires, República Argentina.
Email: matias.braun@ing.unlp.edu.ar

objective of this work is to investigate the effect of ML imperfections on the modal dynamic responses of composite sandwich structures with ML core, using a finite element (FE) model implemented in Abaqus/Standard.[26] A MATLAB algorithm was developed to include the aleatory presence of a certain percentage of imperfections on the lattice structure. In addition, a statistical analysis of the results is presented, in order to define the dependence of the imperfection localisation on the vibration response. The influence of the damage percentage, cell type, cell size and material on the frequency and modal responses of sandwich plates is investigated. The obtained results show that the dynamic frequency responses are dependent on the imperfection (damage) percentage. Therefore, the use of vibration-based NDT methods allows to detect the presence of imperfections on the ML core of sandwich structures.

## Geometrical and material properties

The geometry of the sandwich plate under study is shown in Figure 1. The sandwich structure consisted of unidirectional composite face-sheets and ML core.

The composite face-sheets are made of carbon fibre–reinforced polymer (CFRP) with dimensions of $75 \times 75 \times 1 \, mm^3$, while the core is made of 316L stainless steel[13] with a thickness of 5 mm. There are no restrained degrees of freedom in the sandwich structure.

The material properties of the CFRP face-sheets used in the analysis are $E_x = 140$ GPa, $E_y = E_z = 10$ GPa, $G_{yz} = 3.8$ GPa, $G_{xy} = G_{xz} = 4.6$ GPa, $\nu = 0.25$ and $\rho = 1650 \, kg/m^3$.[27]

It is considered that the ML bar structures exhibit an isotropic linear elastic behaviour with the following material properties: Young's modulus $E = 140$ GPa, Poisson's ratio $\nu = 0.27$ and density $\rho = 7870 \, kg/m^3$.[13,28]

In this study, we considered two unit cell topologies to the ML core: a body-centred cubic (BCC) and the same structure with vertical bar called BCC-Z. Figure 2 shows a schematic representation of the two unit cells.

## Numerical model

The modelling and analysis of free vibration response of sandwich plates are carried out through the commercial FE code Abaqus/Standard.[26] The FE model consists of two parts: composite face-sheets and ML core.

The contact between the different parts is considered to be perfect and modelled using tie constraints, which are implemented in the Abaqus/Standard library.[26] These tie constraints apply a coupling to both displacements and rotations of each pair of interconnected elements of the structure.

The ML core is discretised using simple two-node beam elements to represent the struts in the unit cell,
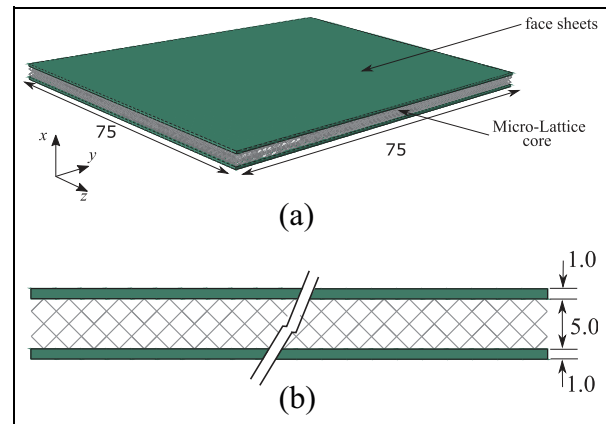


**Figure 1.** Geometry of the sandwich plate (all dimensions are in millimetres): (a) perspective view and (b) side view.

according to the procedure presented by Smith et al.[29] The geometry is simplified, so each strut was represented by a straight beam with a circular cross-section of diameter of 0.20 mm.

In the first place, a comparison between the numerical model in where three-dimensional (3D) elements have been used to mesh the ML core and the numerical model in where the ML core is discretised using simple two-node beam elements is carried out, in order to validate the latter.

Furthermore, in order to validate the core discretisation with beam elements, we implemented other FE model using a 3D element to mesh the ML core. In this case, we used C3D8 elements (continuum 3D reduced integration eight-node elements) to mesh the ML structure.

The free vibration analysis is carried out using linear perturbation load step, obtaining the eigenvalues by means of Lanczos or subspace iteration methods.[26] Influences of imperfection existence on the modal behaviour are discerned by comparisons of dynamic response between a healthy (undamaged) sandwich plate and sandwich plates containing imperfections in the ML core.

Figure 3 presents a general view of FE mesh used to model the sandwich plate. The skins of the sandwich plate are discretised using 45000 C3D8R elements. The FE mesh of the ML core finally accepted due to convergence studies contained approximately 14,398, 36,846 and 48,576 elements for cell sizes ($h$) of 2.5, 1.67 and 1.25 mm, respectively.

The presence of imperfections in the ML core is defined with an algorithm in the MATLAB language. In order to define whether the position of the imperfection affects the dynamic frequency response, we defined the imperfection with a random function. Note that it will be necessary to perform a statistical analysis of the obtained results.

Basically, the MATLAB algorithm defines a random set of elements of the ML core. This set is incorporated within the Abaqus input file and is assigned new
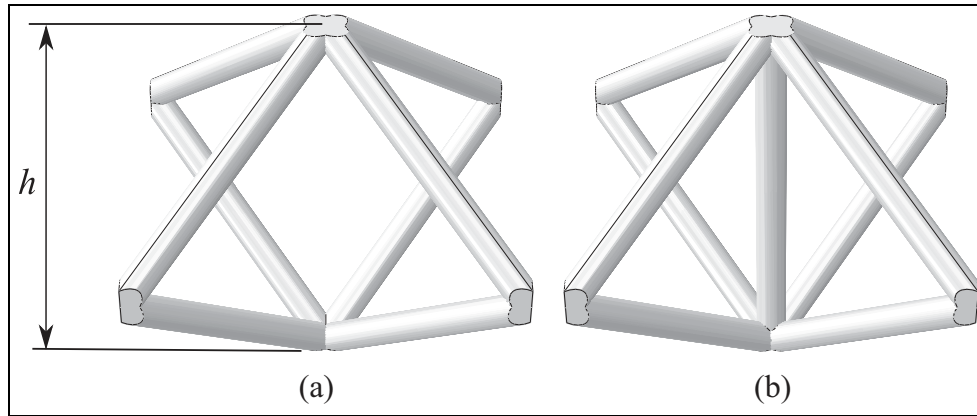
**Figure 2.** Configurations of the unit cells: (a) BCC unit cell and (b) BCC-Z unit cell.
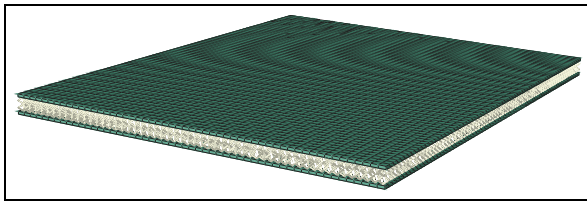


**Figure 3.** Typical mesh of FE model of the sandwich plate.

material properties with null stiffness. Hence, these elements are fictionally vanished from the FE model.

## Results and discussion

In the first place, a comparison between 3D continuum and beam elements is carried out, in order to validate the beam model. Subsequently, a dynamic analysis of the undamaged sandwich structure is presented, showing the most predominant eigenmodes, and the values of the natural frequencies for different cell sizes and cell types. The values of the natural frequencies in the undamaged structure will be used to analyse the influence of damage on the dynamic responses of the sandwich plates.

### Comparison between 3D continuum and beam elements

As mentioned above, in order to reduce the computational cost, a simplified model was developed. This simplified model replaces the 3D elements of the core by simple two-node beam elements to represent the struts in the unit cell.

With the aim to validate the beam model, a comparison between the results obtained with both models was held. This comparison was made by calculating the natural frequencies of vibration, for the two-unit cell topologies considered, obtaining in all cases the percentage error made with the simplified model. These results are shown in Table 1 and Figure 4, considering the first 19 eigenmodes but avoiding those associated with natural

frequencies unlikely to exist. These excluded modes correspond to the torsional modes, which have a complex shape and are difficult to implement in a vibration-based NDT method.

It can be seen that in all cases, the maximum percentage error does not exceed 7.2%. Taking into account all the analysed eigenmodes, the average error for the BCC unit cell is about 2.4%, whereas for the BCC-Z unit cell this average error increases up to 4.3%. Therefore, in view of the results obtained, it can be considered that the beam model is validated and will be used from now on to carry out the subsequent analysis.

### Dynamic analysis of the sandwich structure

In this section, a complete analysis of the dynamic response of the plates is presented, taking into account only those structures with no damage.

As a first result, Figure 5 shows the deformed shape for the first six eigenmodes in sandwich structures with ML core of type BCC. It is important to highlight that the eigenmodes for both types of unit cell for the ML core (i.e. BCC and BCC-Z) are almost identical, showing the corresponding to BCC cell type as an example. Only the first six eigenmodes have been represented because they have the greatest significance in the final deformed shape of the structure, although the first 19 vibration modes have been calculated, as will be corroborated in the following.

With respect to the values of the natural frequencies of vibration, the results are shown by analysing the influence of both the unit cell size and type. As previously stated, two different cell topologies have been considered, the BCC and the BCC-Z. In terms of cell size, three different unit cell sizes have been taken into account: 2.5, 1.67 and 1.25 mm.

In Figure 6, the influence of the cell size can be observed for BCC (Figure 6(a)) and BCC-Z unit cells (Figure 6(b)). In both cases, the first 19 eigenfrequencies have been obtained, omitting those that have a very low probability of appearing. As can be seen, the results for BCC and BCC-Z unit cells are quite similar, with

**Table 1.** Natural frequencies and percentage error obtained with 3D and beam models.

| Mode | BCC | | | BCC-Z | | |
|---|---|---|---|---|---|---|
| | 3D (Hz) | Beam (Hz) | % Error | 3D (Hz) | Beam (Hz) | % Error |
| 1 | 2507.9 | 2470.7 | 1.5 | 2453.0 | 2436.6 | 0.7 |
| 2 | 3712.5 | 3654.7 | 1.6 | 3643.2 | 3629.6 | 0.4 |
| 3 | 5689.8 | 5673.4 | 0.3 | 5575.7 | 5621.0 | 0.8 |
| 4 | 8698.3 | 8870.5 | 2.0 | 8531.8 | 8817.9 | 3.4 |
| 5 | 9093.6 | 9328.2 | 2.6 | 8915.2 | 9268.0 | 4.0 |
| 6 | 9590.2 | 9820.3 | 2.4 | 9409.2 | 9772.9 | 3.9 |
| 7 | 10,121 | 10,344 | 2.2 | 9930.4 | 10,291 | 3.6 |
| 8 | 11,222 | 11,482 | 2.3 | 11,023 | 11,453 | 3.9 |
| 14 | 15,157 | 15,717 | 3.7 | 14,921 | 15,888 | 6.5 |
| 15 | 15,329 | 16,083 | 4.9 | 15,069 | 16,102 | 6.9 |
| 16 | 15,595 | 16,111 | 3.3 | 15,370 | 16,328 | 6.2 |
| 17 | 16,967 | 17,486 | 3.1 | 16,743 | 17,745 | 6.0 |
| 18 | 18,340 | 18,405 | 0.4 | 18,084 | 19,380 | 7.2 |
| 19 | 19,295 | 18,631 | 3.4 | 19,077 | 20,283 | 6.3 |

BCC: body-centred cubic; 3D: three-dimensional.
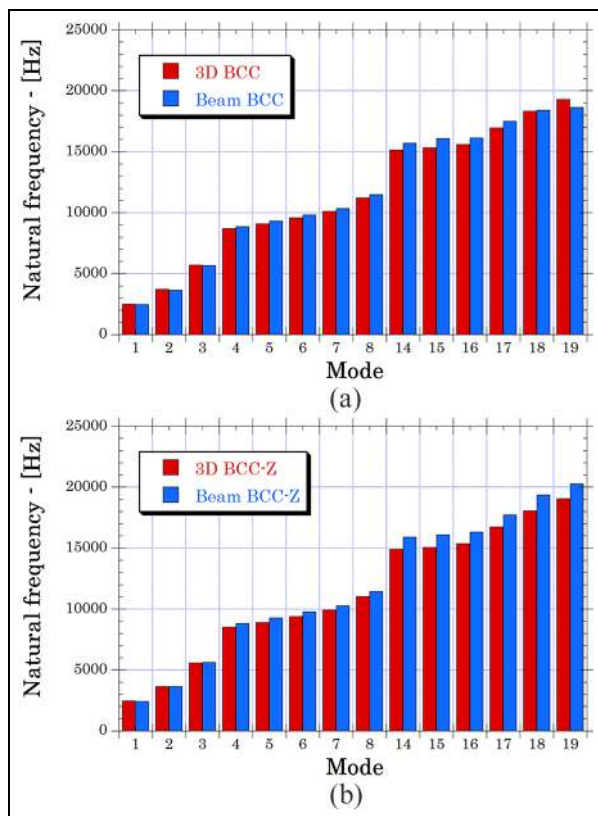


**Figure 4.** Comparison of frequencies between 3D and beam elements: (a) BCC unit cell and (b) BCC-Z unit cell.

both cases following the same trends. The only cell size for which the natural frequencies of vibration always increase with the eigenmodes is 2.5 mm. However, for the immediately smaller cell size (1.67 mm.), some decreases are observed when switching from Mode 6 to Mode 7 and from Mode 14 to Mode 15. Furthermore, when the smallest size (1.25 mm) is analysed, a new decay appears when switching from Mode 17 to Mode 18.

The results comparing the different cell topologies are shown in Figure 7, for each of the considered cell sizes. It is important to note here that for small unit cell sizes, the natural frequencies obtained with the BCC cell core topology are always higher than those corresponding to the BCC-Z topology. However, for the largest of the cell sizes considered, this trend is reversed, observing that for high eigenmodes values, the eigenfrequencies corresponding to the BCC-Z configuration are greater than the corresponding to BCC.

Therefore, as partial conclusions, it can be determined that for small unit cell sizes, the relationship between eigenmodes and the corresponding eigenfrequencies is not always increasing. Furthermore, for these unit cell sizes, the eigenfrequencies in the case of BCC topology are always higher than those for the BCC-Z topology, whereas for the largest of the considered sizes (2.5 mm), this trend is reversed.

## Damage analysis

*Effect of damage localisation.* The damage in the core of the studied sandwich structures was included using an algorithm implemented in MATLAB, which works as follows: after a percentage of damage is selected by the user, the code is executed and programmed to delete a certain number of elements (struts) randomly; thus, for a same percentage of damage, the elements of the core that are removed from the analysis do not necessarily have the same location. As a result, the need to carry out a detailed study of the effect of the damage localisation on the dynamic response of the sandwich structures is readily apparent.

For each eigenmode, the natural frequency was obtained in five simulations with the same damage percentage (from 5% to 40%). Therefore, five values of natural frequency were determined for each case, calculating the standard deviation (SD) and the average
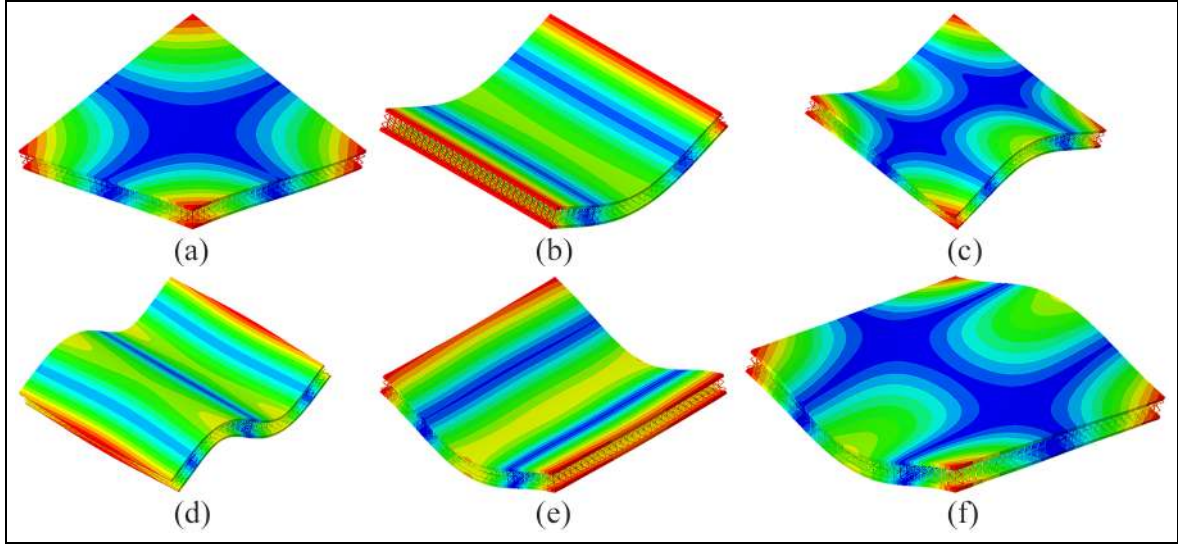
**Figure 5.** Eigenmodes for BCC cell type: (a) Mode 1, (b) Mode 2, (c) Mode 3, (d) Mode 4, (e) Mode 5 and (f) Mode 6.
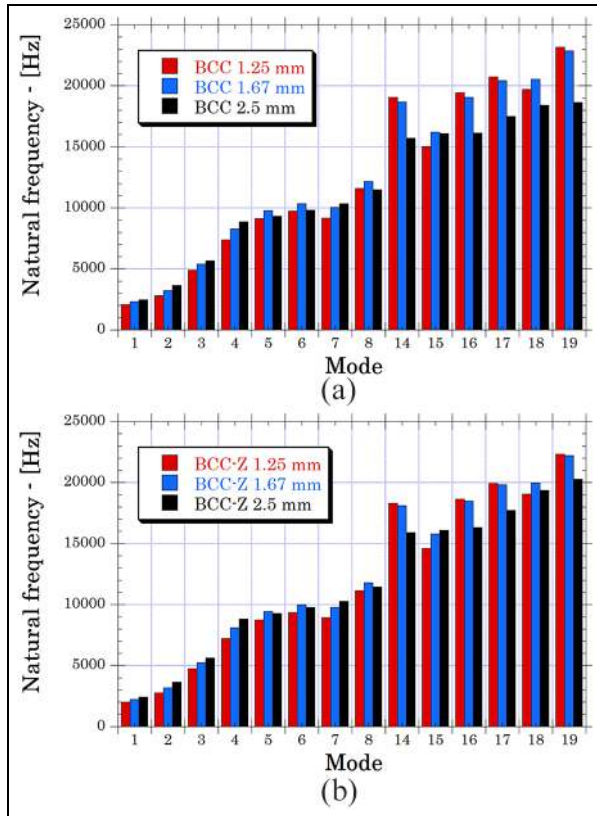


**Figure 6.** Influence of different cell sizes: (a) BCC unit cell and (b) BCC-Z unit cell.

natural frequency (ANF), which results from averaging the five natural frequencies obtained in this section (same eigenmode and same damage percentage). Variations were analysed in terms of the following ratio

$$\text{Standard deviation}_i(\%) = \frac{\text{SD}_i}{\text{ANF}_i} \times 100 \qquad (1)$$

where $i$ corresponds to the studied eigenmode.

The standard deviation ratio as a function of the eigenmode is shown in Figure 8 for each cell type and cell size. For the sake of brevity and since the variations of natural frequencies are more noticeable at higher damage percentages, only results for damage of 40% are presented.

Natural frequencies are more sensitive to damage localisation for larger cell sizes, as results for ML with cell size of 2.5 mm presenting more differences in standard deviation ratio when compared to the ones obtained for cell sizes of 1.25 and 1.67 mm. This is due to the way the algorithm operates to produce damage: removing complete elements (struts). In order to reach the same percentage of damage, fewer struts are deleted in the case of cores with cell size of 2.5 mm than in the case of cell sizes of 1.25 mm. This is due to the size of a single strut in each case. However, deleting less struts produce more localised damage in the structures, and consequently, its influence on the dynamic behaviour of the structure is increased. That is, the larger the cell size, the greater the local effect of damage on the structural response.

In addition, BCC cell type presents more dependence to damage localisation than BCC-Z: although there are similarities between both unit cells, BCC-Z cells are reinforced with vertical struts (see Figure 2) that improve the stability of the core and make it less dependent of damage localisation. In any case, maximum values for standard deviation ratio (for eigenmodes 1–8) are presented in Table 2, in which maximum variations are below 2% in all cases.

As a conclusion, damage localisation does not affect the natural frequencies of the studied sandwich structures. Therefore, in the following sections, ANF will be used in the dynamic analysis of core-damaged sandwich structures.
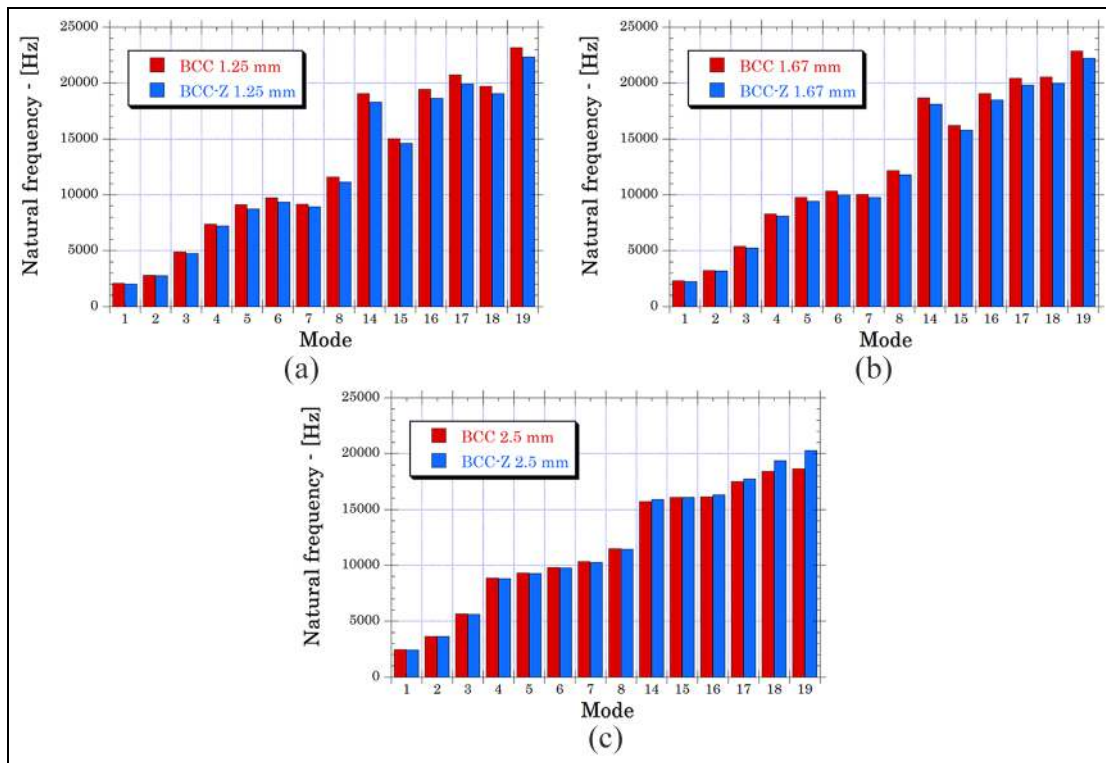
**Figure 7.** Influence of different cell types: (a) 1.25 mm, (b) 1.67 mm and (c) 2.5 mm.
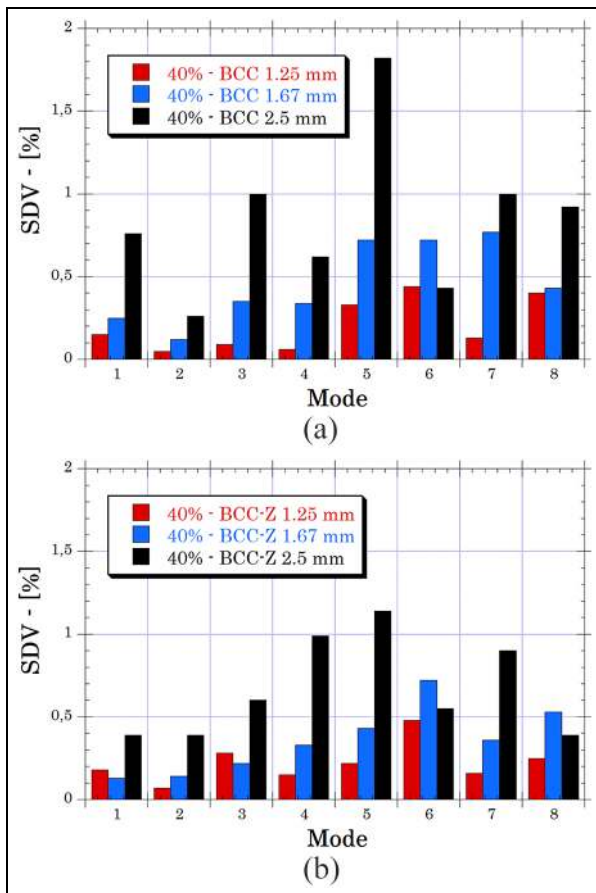


**Figure 8.** Standard deviation as a function of eigenmode: (a) BCC and (b) BCC-Z.

*Effect of damage on eigenmodes.* In order to study the effect of damage on the eigenmodes of sandwich structures, the normalised natural frequency of damaged structures is presented as a function of the selected eigenmodes in Figure 9. As the damage localisation was found to have more influence on cores with greater cell size, results of ML core 2.5 mm are selected for the analysis. The natural frequency of damaged sandwich structures has been normalised with respect to the natural frequency of undamaged structures with the same cell size and type.

Normalised natural frequencies of damaged structures show greater dependence on the eigenmodes for the case of cores with BCC unit cells than for those with BCC-Z cells. This is due to the reinforcement that BCC-Z cells have with respect to the BCC in the form of a central pillar that add stability, as already explained in the previous section. The maximum differences are 35% and 30% for BCC and BCC-Z cores, respectively.

In general, the trends for both cell types are very similar and the effect of damage in the eigenmodes increases with the percentage of damage. In both cell types, the eigenmode with the most influence on the results is number 6; thus, results of the following sections will be presented as a function to this eigenmode.

*Effect of cell size.* Figure 10 shows the effect of the damage on the sandwich structure as a function of the cell size. This figure corresponds to the three sizes studied for both BCC and BCC-Z unit cell types. As stated in

**Table 2.** Maximum standard deviation as a function of cell size, cell type and damage percentage.

| Damage (%) | Size 1.25 mm | | Size 1.67 mm | | Size 2.5 mm | |
|---|---|---|---|---|---|---|
| | BCC | BCC-Z | BCC | BCC-Z | BCC | BCC-Z |
| 5 | 0.07 | 0.06 | 0.13 | 0.19 | 0.33 | 0.27 |
| 10 | 0.13 | 0.16 | 0.24 | 0.30 | 0.29 | 0.36 |
| 15 | 0.14 | 0.14 | 0.35 | 0.29 | 0.44 | 0.58 |
| 20 | 0.12 | 0.17 | 0.55 | 0.34 | 1.16 | 0.54 |
| 25 | 0.18 | 0.20 | 0.67 | 0.45 | 0.68 | 0.61 |
| 30 | 0.25 | 0.20 | 0.61 | 0.49 | 1.19 | 0.96 |
| 35 | 0.42 | 0.25 | 0.82 | 0.45 | 1.20 | 1.39 |
| 40 | 0.44 | 0.48 | 0.77 | 0.72 | 1.82 | 1.14 |

BCC: body-centred cubic.
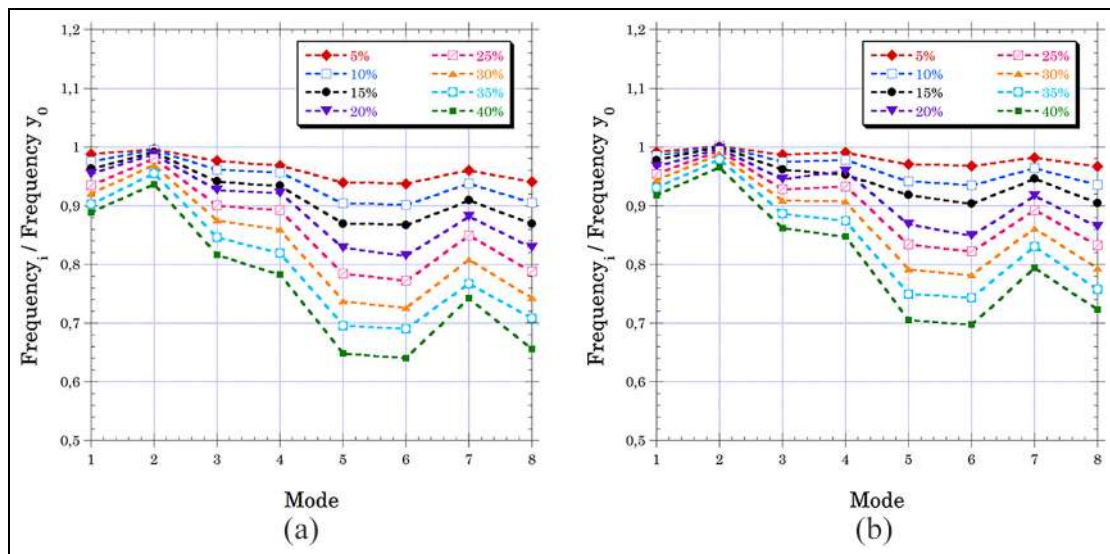


**Figure 9.** Normalised frequencies versus damage: (a) BCC and (b) BCC-Z.
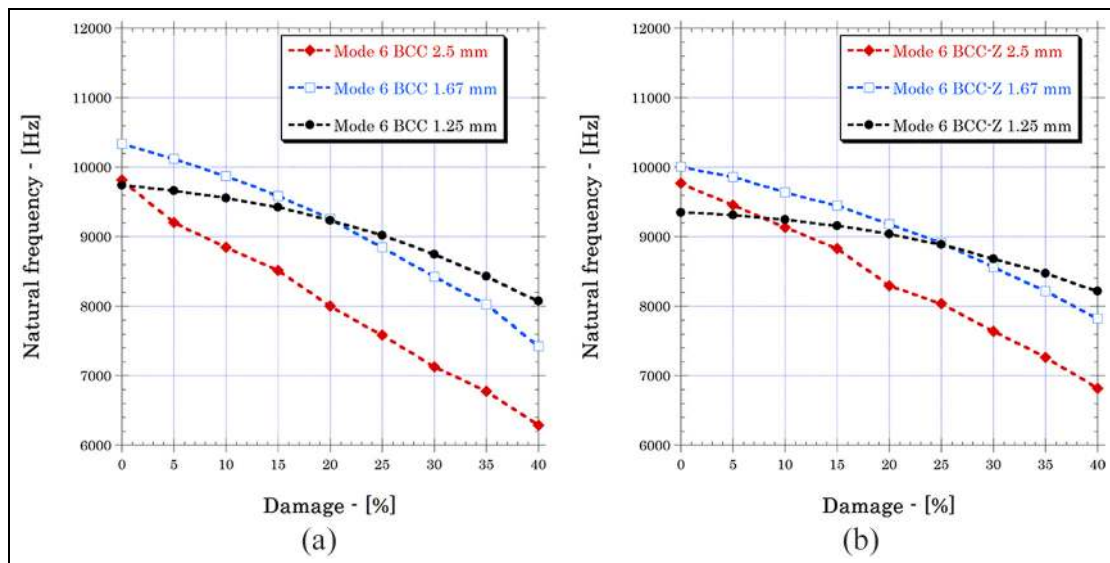


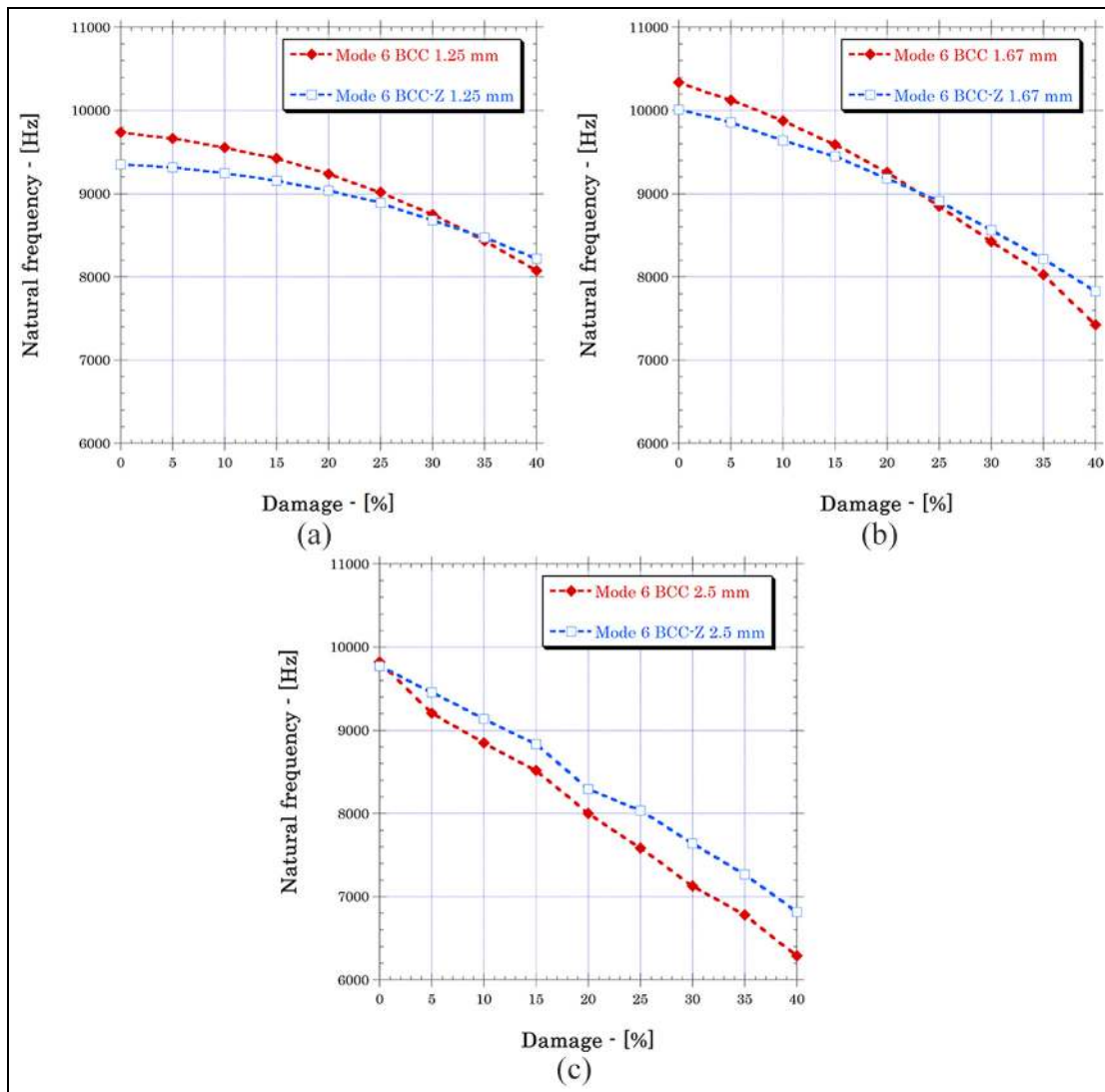**Figure 10.** Frequencies versus damage for different cell sizes: (a) BCC and (b) BCC-Z.

**Figure 11.** Frequencies versus damage for different cell types: (a) 1.25 mm, (b) 1.67 mm and (c) 2.5 mm.

the previous section, only results for eigenmode 6 are shown, since it is the eigenmode in which the influence of the damage is more noticeable. Variations are again more visible for results of structures with BCC cells than for BCC-Z.

Natural frequency decreases with increasing percentage of damage for the three sizes. For less damage level, cells of 1.67 mm show greater frequencies when compared to cells of 2.5 and 1.25 mm. However, this trend changes when a certain damage level is reached, and cores with cells of smaller size (1.25 mm) present less changes in the natural frequency with the augmenting of damage. The greatest differences are shown for larger cells (2.5 mm), in which the decrease is almost linear with damage. These results are explained in a similar way to those presented in section 'Effect of damage localisation': as the level of damage increases, cores with smaller unit cells distribute removed struts more homogeneously. Thus, cores with greater cell sizes are more affected by damage.

*Effect of cell type.* Comparison of natural frequency as a function of damage for each cell type is shown in Figure 11. As previously stated, differences between natural frequencies (from undamaged cores to 40% of damage level) are more noticeable in BCC results than in BCC-Z due to their structural arrangement.

Trends are similar for both unit cells. For cell size of 2.5 mm, natural frequencies are always higher for BCC-Z cells; however, for the smallest cell size (1.25 mm), natural frequencies are higher in BCC results up to a damage level of 35%, in which BCC results are slightly lower than BCC-Z. For cell sizes of 1.67 mm, BCC natural frequencies are lower than the ones given for BCC-Z from damage level of 25%.

*Effect of cell material types.* In order to analyse the effect of the micro-lattice core material on the free vibration response, it has been considered two simply supported square plates of approximately the same weight but
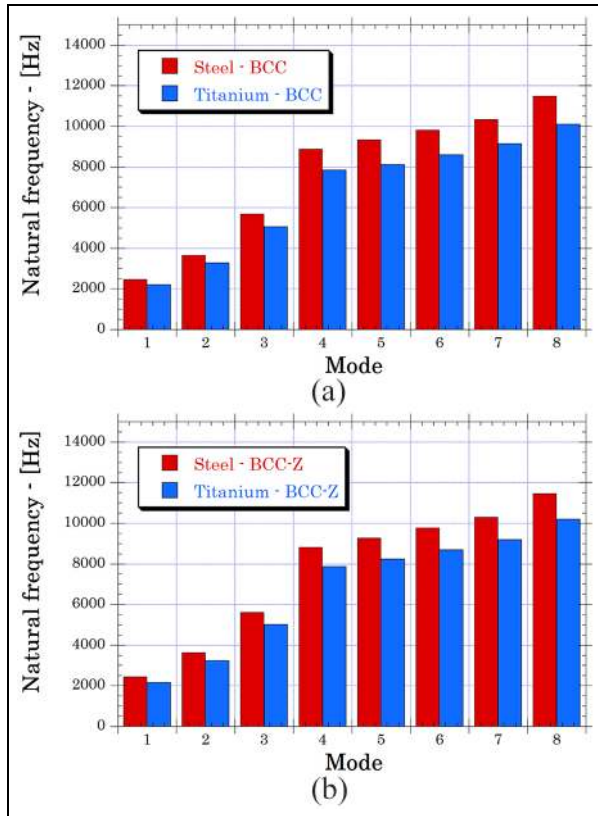
**Figure 12.** Natural frequencies for undamaged specimens. Steel versus titanium cell core: (a) BCC and (b) BCC-Z.

different ML core materials: stainless steel 316L and titanium alloy Ti-6Al-4V.[30]

The mechanical properties of the Ti-6Al-4V used in this analysis are Young's modulus $E = 45$ GPa, Poisson's ratio $\nu = 0.30$ and density $\rho = 4680$ kg/m³.[14]

In this study, only the core cell size of 2.50 mm has been considered, for both cell materials. The diameter of the struts adopted for the ML core of Ti-6Al-4V is 0.35 mm, whereas that adopted for the stainless steel 316L is 0.20 mm, in agreement with the work presented by Mines et al.[14] In first place, the natural frequencies on undamaged sandwich structures have been analysed, for both core materials and for the two topologies previously studied (Figure 12).

Results for both cell types and materials show similarities. As it was presented in previous sections, the natural frequency increases with increasing eigenmode number. Natural frequencies for sandwich structures with titanium ML core are lower than those obtained for steel core structures. In general, natural frequency is proportional to the square root of the stiffness (controlled by Young's modulus of the material) and inversely proportional to the square root of the mass (controlled by the density). Steel has Young's modulus of 68% higher than the one given for the titanium, while its density is just 40% higher; therefore, natural frequencies for steel ML cores are higher than the ones obtained for ML cores made of titanium.

Figure 13 presents the normalised natural frequency of damaged sandwich structures with titanium ML core. For both BCC and BCC-Z cell types, eigenmode number 6 is the more affected by the presence of damage, which coincides with results obtained for steel cores.

Once the eigenmode that is most affected by the presence of damage has been identified for both materials, a comparison of how damage growth affects the natural frequencies for the two cell types studied as a function of the material is presented in Figure 10. As previously stated, steel cores show higher natural frequencies in all cases due to its higher properties, particularly the value of Young's modulus. In BCC structural arrangement, natural frequencies for steel are more affected by the presence of damage than in the case of titanium, as differences between the natural frequency without damage (damage of 0%) and natural
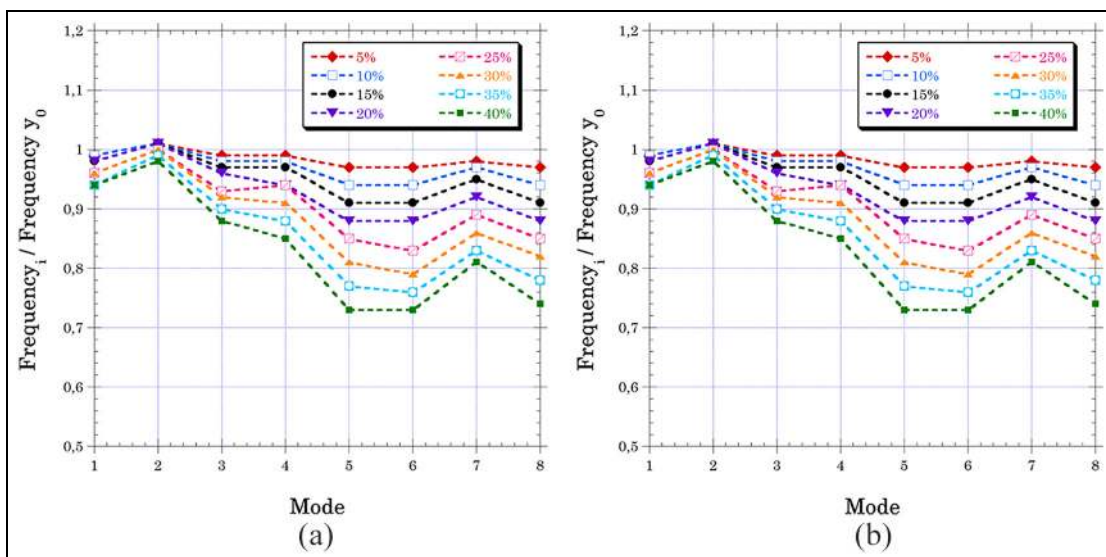


**Figure 13.** Normalised frequencies versus damage for titanium cell core: (a) BCC and (b) BCC-Z.
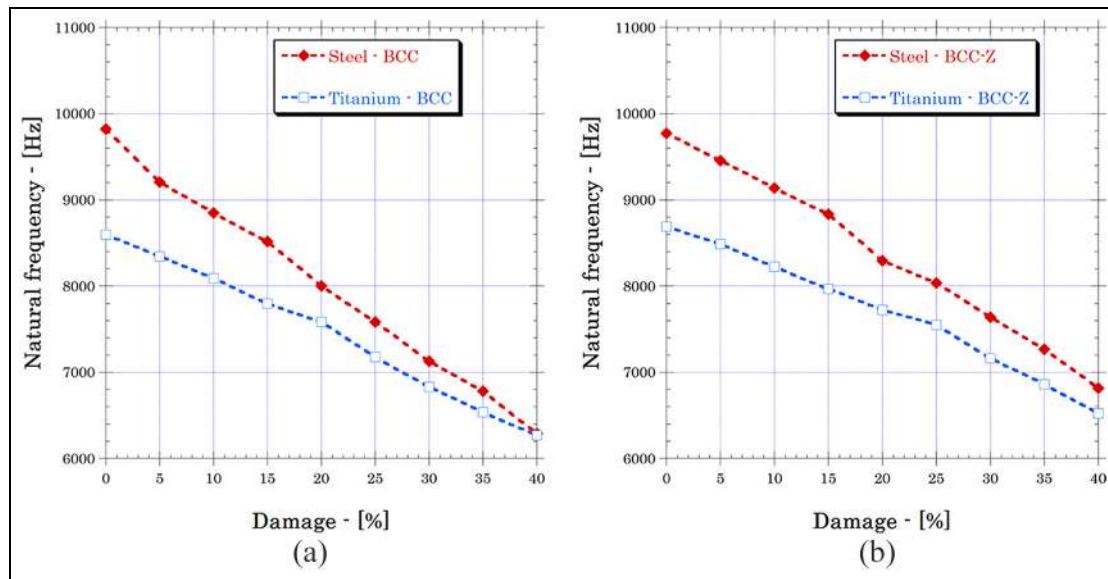
**Figure 14.** Frequencies of the eigenmode number 6 versus damage for different cell materials: (a) BCC and (b) BCC-Z.

frequency with a damage level of 40% are 36% and 27% for steel and titanium, respectively (Figure 14(a)). For BCC-Z cell type, natural frequencies of steel and titanium decrease at a similar rate with augmenting damage level of 30% and 25%, respectively. As a conclusion, the dynamic behaviour of BCC-Z ML cores is less affected by the properties of the material used in its manufacture.

## Conclusion

In this work, we implemented an FE model to study the dynamic frequency responses of sandwich plates with ML metallic core. The simulations are focused to show the sensitivity of the dynamic responses with the presence of defects in the ML core. In this way, we developed a MATLAB code to generate random defects in the ML core.

We presented an extensive parametric study, where we analysed the effect of localisation defects, cell sizes, cell types and cell material types. The following points are the principal conclusions from this analysis:

- Natural frequencies are more sensitive to damage localisation for larger cell sizes. Furthermore, the BCC unit cell type presents more dependence to damage localisation than BCC-Z. However, the damage localisation does not affect significantly the natural frequencies of the studied sandwich plates.
- For BCC and BCC-Z cells, the effect of damage in the eigenmodes increases with the percentage of damage. In both cell types, the eigenmode with the most influence on the results is number 6.
- The dynamic response of the sandwich structures with greater cell sizes is more affected by damage.
- The natural frequencies present the same tendency for both types of unit cells.

- Natural frequencies for sandwich structures with titanium ML core are lower than those obtained for steel core structures.

Therefore, we could conclude that NDT based on vibration analysis can be an interesting tool to detect the damage of sandwich plates with ML cores. However, future works are required to validate our numerical results with experimental data. Furthermore, we can study the sensitive of the mechanical properties with the presence of defects in ML blocks.

### Declaration of conflicting interests

The author(s) declared no potential conflicts of interest with respect to the research, authorship, and/or publication of this article.

### ORCID iD

Matías Braun https://orcid.org/0000-0003-4689-0822

### References

1. Soden PD. Indentation of composite sandwich beams. *J Strain Anal Eng* 1996; 31(5): 353–360.

2. Kamiya N. Analysis of the large thermal bending of sandwich plates by a modified Berger method. *J Strain Anal Eng* 1978; 13(1): 17–22.

3. Holt PJ and Webber JPH. Exact solutions to some honeycomb sandwich beam, plate, and shell problems. *J Strain Anal Eng* 1982; 17(1): 1–8.

4. Udatha P, Kumar CVS, Nair NS, et al. High velocity impact performance of three-dimensional woven composites. *J Strain Anal Eng* 2012; 47(7): 419–431.

5. Vinson J. *The behavior of sandwich structures of isotropic and composite materials*. London: Routledge, 2018.

6. Heimbs S, Cichosz J, Klaus M, et al. Sandwich structures with textile-reinforced composite foldcores under impact loads. *Compos Struct* 2010; 92(6): 1485–1497.

7. Lolive É and Berthelot JM. Non-linear behaviour of foam cores and sandwich materials, part 2: indentation and three-point bending. *J Sandw Struct Mater* 2002; 4(4): 297–352.

8. Berthelot JM and Lolive É. Non-linear behaviour of foam cores and sandwich materials, part 1: materials and modelling. *J Sandw Struct Mater* 2002; 4(3): 219–247.

9. Sypeck DJ. Cellular truss core sandwich structures. *Appl Compos Mater* 2005; 12(3–4): 229–246.

10. Queheillalt DT and Wadley HN. Titanium alloy lattice truss structures. *Mater Design* 2009; 30(6): 1966–1975.

11. Rashed M, Ashraf M, Mines R, et al. Metallic microlattice materials: a current state of the art on manufacturing, mechanical properties and applications. *Mater Design* 2016; 95: 518–533.

12. Gümrük R, Mines R and Karadeniz S. Static mechanical behaviours of stainless steel micro-lattice structures under different loading conditions. *Mat Sci Eng A-Struct* 2013; 586: 392–406.

13. Tsopanos S, Mines R, McKown S, et al. The influence of processing parameters on the mechanical properties of selectively laser melted stainless steel microlattice structures. *J Manuf Sci E-T ASME* 2010; 132(4): 041011.

14. Mines R, Tsopanos S, Shen Y, et al. Drop weight impact behaviour of sandwich panels with metallic micro lattice cores. *Int J Impact Eng* 2013; 60: 120–132.

15. Jacobsen AJ, Barvosa-Carter W and Nutt S. Compression behavior of micro-scale truss structures formed from self-propagating polymer waveguides. *Acta Mater* 2007; 55(20): 6724–6733.

16. Cansizoglu O, Harrysson O, Cormier D, et al. Properties of Ti-6Al-4V non-stochastic lattice structures fabricated via electron beam melting. *Mat Sci Eng A-Struct* 2008; 492(1–2): 468–474.

17. Hasan R, Mines R and Tsopanos S. Determination of elastic modulus value for selectively laser melted titanium alloy micro-struty. *J Mech Eng Technol* 2010; 2(2): 17–25.

18. Doebling SW, Farrar CR, Prime MB, et al. Damage identification and health monitoring of structural and mechanical systems from changes in their vibration characterisics: a literature review. *Technical Report, Los Alamos National Lab, Los Alamos, NM,* 1 May 1996.

19. Yang Z, Wang L, Wang H, et al. Damage detection in composite structures using vibration response under stochastic excitation. *J Sound Vib* 2009; 325(4): 755–768.

20. Kwon Y and Lannamann D. Dynamic numerical modeling and simulation of interfacial cracks in sandwich structures for damage detection. *J Sandw Struct Mater* 2002; 4(2): 175–199.

21. Duc ND, Cong PH, Tuan ND, et al. Nonlinear vibration and dynamic response of imperfect eccentrically stiffened shear deformable sandwich plate with functionally graded material in thermal environment. *J Sandw Struct Mater* 2016; 18(4): 445–473.

22. Saraswathy B, Mangal L and Kumar RR. Analytical approach for modal characteristics of honeycomb sandwich beams with multiple debond. *J Sandw Struct Mater* 2012; 14(1): 35–54.

23. Elmalich D and Rabinovitch O. On the effect of interlaminar contact on the dynamics of locally delaminated FRP strengthened walls. *Int J Nonlin Mech* 2015; 77: 141–157.

24. Zou Y, Tong L and Steven G. Vibration-based model-dependent damage (delamination) identification and health monitoring for composite structures – a review. *J Sound Vib* 2000; 230(2): 357–378.

25. Farrar CR and Worden K. An introduction to structural health monitoring. *Philos T Roy Soc A* 2007; 365(1851): 303–315.

26. ABAQUS/Standard. *Abaqus standard v6.13 user's manual*, version 6.13. Richmond. VA: ABAQUS Inc, 2013.

27. Burlayenko VN and Sadowski T. Influence of skin/core debonding on free vibration behavior of foam and honeycomb cored sandwich plates. *Int J Nonlin Mech* 2010; 45(10): 959–968.

28. Ushijima K, Cantwell W, Mines R, et al. An investigation into the compressive properties of stainless steel microlattice structures. *J Sandw Struct Mater* 2011; 13(3): 303–329.

29. Smith M, Guan Z and Cantwell W. Finite element modelling of the compressive response of lattice structures manufactured using the selective laser melting technique. *Int J Mech Sci* 2013; 67: 28–41.

30. Polmear I. *Light alloys: from traditional alloys to nanocrystals*. Amsterdam: Elsevier, 2005.